Molecular Vision 2026; 32:410-419 <http://www.molvis.org/molvis/v32/410>
Received 5 November 2025 | Accepted 14 September 2026 | Published 20 September 2026

© 2026 Molecular Vision

Clinicogenetic insights in Indian patients with cornea plana: A case series from India with novel *KERA* variants

Anshuman Verma,[1] Sneha Pranahitha Gorenka,[1] Sunita Chaurasia,[1,2,3] Deepak P. Edward,[4] Muralidhar Ramappa[1,2,3]

[1]Institute for Rare Eye Diseases and Ocular Genetics, L V Prasad Eye Institute, Hyderabad, India; [2]Cornea Institute, L V Prasad Eye Institute, Hyderabad, India; [3]Jasti V Ramanamma Children's Eye Care Center, L V Prasad Eye Institute, Hyderabad, India; [4]Department of Ophthalmology, King Khaled Eye Specialist Hospital, Riyadh, Saudi Arabia

Purpose: Cornea plana (CP) is a rare congenital anterior segment anomaly characterized by markedly flat corneal curvature under the influence of the *KERA* gene variant. The present study aims to delineate the clinical phenotype and underlying *KERA* gene variants in Indian patients with CP and to expand the mutational and phenotypic landscape of this rare congenital corneal dystrophy.

Methods: A retrospective study was performed for seven pediatric patients diagnosed with CP between 2010 and 2024 at a tertiary eye care center in India. All patients underwent comprehensive ophthalmic examinations. Whole-exome sequencing was conducted in all probands to detect pathogenic variants, which were classified according to the American College of Medical Genetics and Genomics guidelines and further assessed using in silico predictive tools.

Results: All seven cases exhibited the hallmark features of autosomal recessive CP, including bilateral microcornea, markedly flattened corneas, stromal haze, high hyperopia, indistinct limbal zone, and shallow anterior chamber. Iris adhesions were observed in six of seven patients. Genetic analysis revealed that all six probands harbored distinct homozygous *KERA* variants: two novel frameshift variations, c.264_298del (p.Glu88Aspfs*14) and c.59_78delinsA (p.Ser20TyrfsTer57); two known stop-gain variations, c.937C>T (p.Arg313Ter) and c.835C>T (p.Arg279Ter); and two known missense variations, c.809C>T, (p.Ser270Leu) and c.528C>G (p.Asn176Lys). One family with CP demonstrated a pseudo-dominant inheritance pattern evident from multiple affected members history despite molecular confirmation of a homozygous *KERA* variant in the proband. Management included refractive correction, occlusion therapy for amblyopia, and selective anterior segment reconstruction, including pupilloplasty in one eye and synechiolysis in another case. Despite these interventions, visual outcomes remained limited.

Conclusions: This study expands the clinical and genetic spectrum of *KERA*-associated CP in an Indian cohort by identifying two novel variants and documenting a rare pseudo-dominant inheritance pattern. Visual outcomes were generally limited, likely attributable to delayed presentation and amblyopia secondary to uncorrected high hyperopia during the critical period of neuroplasticity. Early recognition, prompt refractive correction, and molecular confirmation are essential to optimize visual prognosis and enable appropriate genetic counseling.

Cornea plana (CP) is a rare congenital anterior segment anomaly characterized by markedly reduced corneal curvature, which leads to an abnormally flat corneal surface. This results in decreased refractive power (25–35 D compared to the physiologic range of 40–45 D) and frequently coexists with microcornea, shallow anterior chamber, and central or peripheral corneal opacification [1]. Clinically, CP may present in early childhood with severe hyperopia, esotropia, and reduced visual acuity. The corneal limbus is typically widened and hazy, and a prominent arcus lipoides may be observed. In CP, the overall corneal thickness is reduced, with the periphery thinner than the center, a reversal of the distribution of corneal thickness in normal eyes, resulting in optical and structural impairments [2].

CP can manifest as either an autosomal dominant (CNA1; OMIM 121400) or autosomal recessive trait (CNA2; OMIM 217300) [3]. While the dominant form tends to be mild and manageable with optical correction, the recessive variant presents with greater anatomic derangement and often requires surgical intervention. Severe forms of CNA2 may involve anterior segment dysgenesis, including iris hypoplasia, correctopia, posterior embryotoxon, iris adhesions, and iris strands arising from the iris collarette and inserted onto the posterior surface of the cornea. These manifestations may lead to complications such as corneal ectasia, glaucoma, cataracts, and amblyopia [4]. Notably, CP may phenotypically overlap with other congenital corneal opacities, such as peripheral sclerocornea, posterior amorphous corneal dystrophy, and connective tissue disorders, such as

Correspondence to: Muralidhar Ramappa, Head, Institute for Rare Eye Diseases and Ocular Genetics. The Cornea Institute & Jasti V Ramanamma Children's Eye Care Center, L V Prasad Eye Institute, Hyderabad, Telangana, India; Phone: +91 40 681012623, FAX: +91 40 68108271; email: muralidhar@lvpei.org.

Ehlers-Danlos syndrome type VI, making its accurate diagnosis a clinical challenge [5,6]. Advanced diagnostics, such as corneal topography, anterior segment optical coherence tomography (AS-OCT), and genetic testing, are instrumental in confirming the diagnosis and distinguishing CP from other similar disorders.

Genetically, autosomal recessive CP (CNA2) is linked to pathogenic variants of the *KERA* gene located on chromosome 12q22 [7]. *KERA* is a member of the small leucine-rich proteoglycan family and encodes keratocan, a cornea-specific keratan sulfate proteoglycan that is essential for maintaining the structural organization and optical transparency of the corneal stroma [8]. Loss of function in *KERA* disrupts collagen fibril alignment and stromal architecture, resulting in a CP phenotype as demonstrated in *KERA* knockout mice [9].

Although *KERA*-associated CP has been well characterized in Finnish and Saudi populations, often due to founder effects and high rates of consanguinity, reports from other ethnic backgrounds remain limited [1,10]. Most reported *KERA* variants are confined to a small number of recurrent variations, and little is known about the genetic diversity of CP in non-European populations. Data from underrepresented regions, such as India, are crucial for expanding the current understanding of genotype–phenotype correlations and allelic heterogeneity in CP.

In this study, we present one of the larger case series of genetically confirmed CP reported from India to date. This study provides insights into the phenotypic variability, inheritance patterns, and mutational spectrum of CP in a previously underrepresented Indian population.

METHODS

Study design and participants: This retrospective study was conducted at the L V Prasad Eye Institute, Hyderabad, India, after approval from the institutional review board and in accordance with the Declaration of Helsinki. Medical records of pediatric patients diagnosed with CP between January 2010 and December 2024 were reviewed. Written informed consent for the use of clinical and genetic data was obtained from the parents or legal guardians at the time of registration.

Inclusion criteria comprised pediatric patients diagnosed with CP based on characteristic clinical findings, including microcornea, markedly flattened corneal curvature, corneal opacification or stromal haze, indistinct limbal architecture, and iris adhesions or shallow anterior chambers. Patients with isolated microcornea or nonspecific corneal haze without supportive clinical features, or those with incomplete ophthalmic or genetic records, were excluded. A total of seven cases, including six probands (CP1–CP6) and one affected sibling (CP5a), fulfilled the eligibility criteria and were included in the analysis.

Clinical evaluation: Demographic and clinical data were extracted from electronic medical records. Variables recorded included age at presentation, sex, laterality, parental consanguinity, family history, and clinical presentation wherever available, such as visual acuity, refractive error, keratometry values, axial length, anterior segment findings, and intraocular pressure. All patients underwent ophthalmic examination, including slit-lamp biomicroscopy, cycloplegic retinoscopy, and dilated fundus examination when media clarity permitted. Anterior segment imaging was performed using AS-OCT or ultrasound biomicroscopy (UBM) to assess corneal thickness, anterior chamber depth, angle configuration, and iris insertion. AS-OCT was performed in CP1, CP5, and CP5a, whereas UBM was performed in the remaining cases. Corneal endothelial specular microscopy was performed in CP5a.

Genetic analysis: Whole-exome sequencing was performed in all probands (CP1–CP6) at a certified molecular diagnostics laboratory (Redcliffe Labs, Hyderabad, India) to identify pathogenic variants in *KERA*. Exome capture targeted approximately 99% of protein-coding regions (CCDS and RefSeq databases). Sequencing was performed on the Illumina NovaSeq platform (San Diego, CA, USA) with an average coverage depth of 100–150×; >90% of targeted regions achieved ≥30× coverage. Variant calling was performed using the Genome Analysis Toolkit, and annotation was conducted using Golden Helix VarSeq and VarSome pipelines. Variants were interpreted according to the American College of Medical Genetics and Genomics guidelines, as provided in the laboratory report.

In silico and structural analysis: Pathogenicity of identified variants was evaluated using multiple in silico prediction tools. Variant annotation and functional prediction were performed using Ensembl Variant Effect Predictor (VEP) and MutationTaster. Functional impact was further assessed using SIFT, PolyPhen-2, and combined annotation-dependent depletion (https://cadd.gs.washington.edu/) scores. Predictions of nonsense-mediated mRNA decay were also analyzed. Evolutionary conservation of altered amino acid residues was assessed across orthologous species using multiple sequence alignment with Clustal Omega. A homology-based three-dimensional model of the wild-type (WT) human KERA protein was generated using MODELER, employing the crystal structure of the fused N-terminal domains of Internalin B (PDB ID: 1H6T) as the template. Mutant protein

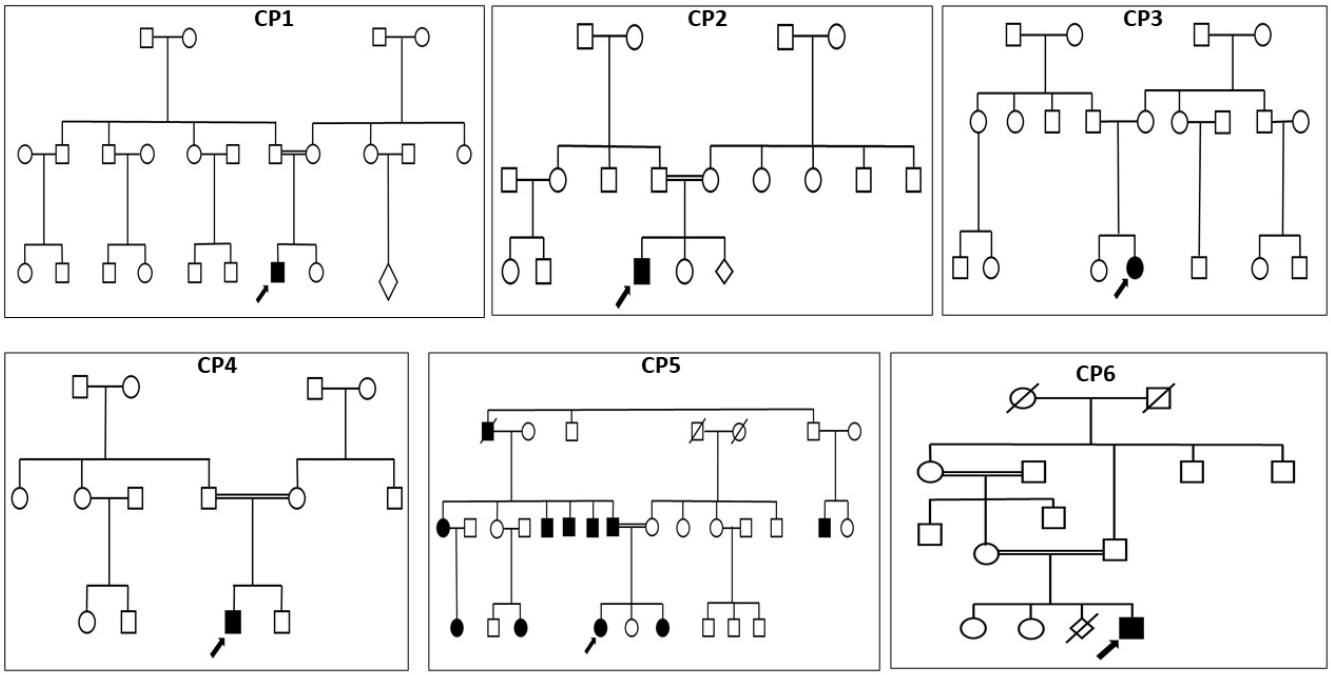


Figure 1. Pedigree of six cornea plana (CP) cases. All pedigrees indicate autosomal recessive inheritance in indexed cases. The CP5 pedigree illustrates multiple affected individuals across generations, suggestive of pseudo-dominant inheritance.

models (p.Asn176Lys and p.Ser270Leu) were generated based on the WT structure. Structural superimposition and root mean square deviation analysis were performed using UCSF Chimera. Changes in protein stability (ΔΔG) between WT and mutant proteins were estimated using DDMut.

RESULTS

Demographic and clinical characteristics: Seven children (four males, three females) with clinically diagnosed CP were included. The mean age at presentation was 1.9 years. Bilateral involvement was observed in all cases. Parental consanguinity was documented in five of six families (83%). A positive family history was present in one family (CP5), in which the sibling (CP5a) exhibited a similar phenotype (Figure 1). Presenting visual acuity was markedly reduced, ranging from fix-and-follow behavior in infants (CP2, CP3, and CP6) to measurable acuity in a ranging from 6/36 to 6/201 in older children (CP1, CP4, CP5, CP5a). High hyperopia (+9.5 to +14.0 D) was observed in all patients. Intraocular pressure was within normal limits in all except CP1, who had elevated pressures (25–26 mm Hg). Slit-lamp examination revealed microcornea, markedly flattened corneal curvature, indistinct limbal architecture, and central or diffuse stromal haze in all cases. Anterior segment imaging (AS-OCT/UBM) consistently demonstrated anterior iris insertion in all except one (CP4), and all eyes exhibited shallow anterior chambers (Table 1). The representative images of ocular presentation are shown in Figure 2 and Figure 3 for CP1 and CP5a, respectively. Fundus evaluation (image not shown) was feasible in four cases (CP1, CP3, CP4, CP6); optic discs were normal in three, whereas CP1 showed glaucomatous cupping consistent with secondary glaucoma. Visualization was not possible in other cases due to dense corneal haze, obliterated pupils, or noncooperation.

Management and visual outcomes: Given the late presentation and absence of prior adequate visual rehabilitation, dense amblyopia was already established in these patients. Therefore, all patients received high-plus refractive correction and occlusion therapy. Surgical intervention was required in two patients: pupilloplasty in one eye of CP1 and synechiolysis in CP3. The surgical interventions in CP1 were primarily performed to enlarge the pupillary aperture to facilitate accurate refraction and fundus visualization and in CP3 to reduce the risk of secondary developmental glaucoma. CP1 also required topical antiglaucoma medication owing to glaucomatous features. Eyes undergoing surgical intervention (in

Table 1. Clinical, imaging, and genetic characteristics of cornea plana.

S. No. (Row)	Column	Current	Correct
1 (CP1)	BCVA @ presentation (OS)	6//180	6/180
1 (CP1)	Keratometry	Kavg=35.	Kavg = 35
3 (CP3)	Slit-lamp findings	Microcornea Mild Haze	Microcornea, Mild haze
4 (CP4)	Slit-lamp findings	Indistinct flat limbus,	Indistinct limbus
5 (CP5)	Keratometry	Kavg=36.	Kavg = 36
6 (CP5a)	Final BCVA	OD: 20/200	OD: 6/60
		Os: 20/50	OS: 6/15
1–7 (All rows)	AS-OCT/UBM findings	Mixed use of periods	Use one punctuation style consistently (preferably no full stop at the end of table-cell entries).

This table summarizes the patient demographic variables, clinical features, refractive status, corneal biometric readings, slit lamp and anterior segment image (UBM/AS-OCT) findings of the 7 children diagnosed with CP. All patients exhibited flat corneal curvature and findings consistent with CP.

CP1 and CP3) demonstrated modest visual improvement, with gains of up to one Snellen line from baseline acuity. Patients managed conservatively (CP2, CP4–CP7) with early optical correction maintained functional visual acuity ranging from 6/9 to 6/240 at final follow-up (Table 1).

Genetic findings: Homozygous *KERA* variants (NM_007035.4) were identified in all six probands (Table 2). Two novel frameshift variants were detected: c.264_298del (p.Glu88Aspfs*14) in CP1 and c.59_78delinsA (p.Ser20TyrfsTer57) in CP2. CP3 harbored a missense variant, c.809C>T (p.Ser270Leu); CP4 carried a stop-gain (nonsense) variant, c.937C>T (p.Arg313Ter); CP5 exhibited a missense variant, c.528C>G (p.Asn176Lys); and CP6 carried a stop-gain variant, c.835C>T (p.Arg279Ter)—all documented previously in CP. The CP5 pedigree suggested pseudo-dominant inheritance due to multiple affected individuals across generations despite an underlying autosomal recessive genotype (Figure 1).

In silico and structural analysis: In silico analysis supported pathogenicity for most identified variants (Table 2). The frameshift variants were predicted to result in premature truncation with likely nonsense-mediated decay. The Mutation Taster identified all variants to be deleterious. The nonsense variants p.Arg313Ter and p.Arg279Ter were predicted to escape nonsense-mediated decay, potentially producing truncated proteins. The missense variants (p.Ser270Leu and p.Asn176Lys) were predicted to be deleterious by SIFT, PolyPhen-2, and combined annotation-dependent depletion. Conservation analysis demonstrated strong evolutionary conservation at the Asn176 and Ser270 positions (Figure 4). Structural modeling of mutant proteins (p.Asn176Lys and p.Ser270Leu) (Figure 5B) revealed minimal global conformational deviation between wild-type and mutant proteins (root mean square deviation 0.188 Å and 0.204 Å, respectively). However, stability analysis predicted destabilization (mutation cutoff scanning matrix [mCSM] ΔΔG −0.16 kcal/mol; site-directed mutator [SDM] ΔΔG −1.33 kcal/mol), suggesting functional impairment despite preservation of overall protein folding.

DISCUSSION

This study reports six genetically confirmed cases of CP of Indian origin, each harboring homozygous pathogenic or likely pathogenic variants of the *KERA* gene. Our findings not only confirm the clinical diagnosis but also expand the known mutational spectrum associated with CP. Although CP has been historically reported in populations from Finland, Cuba, and Saudi Arabia, data from ethnically diverse groups remain limited [1,10,11]. To the best of our knowledge, this study presents one of the most extensive clinically and genetically characterized series of CP cases from India, contributing to a better understanding of its phenotypic variability and genetic diversity.

All patients in our cohort presented with the features of CP, including bilateral microcornea, markedly flattened corneal curvature, and stromal opacification involving the visual axis. Associated anterior segment findings, such as iris adhesions, anterior chamber shallowing, and pupillary displacement, were observed. These structural abnormalities frequently lead to profound visual impairment, ranging from fix-and-follow behavior to severe amblyopia and high hyperopia. Published literature offers limited documentation of iris adhesions in CP. Bruni et al. [12] described a single case demonstrating iris synechiae using laser-scanning in vivo

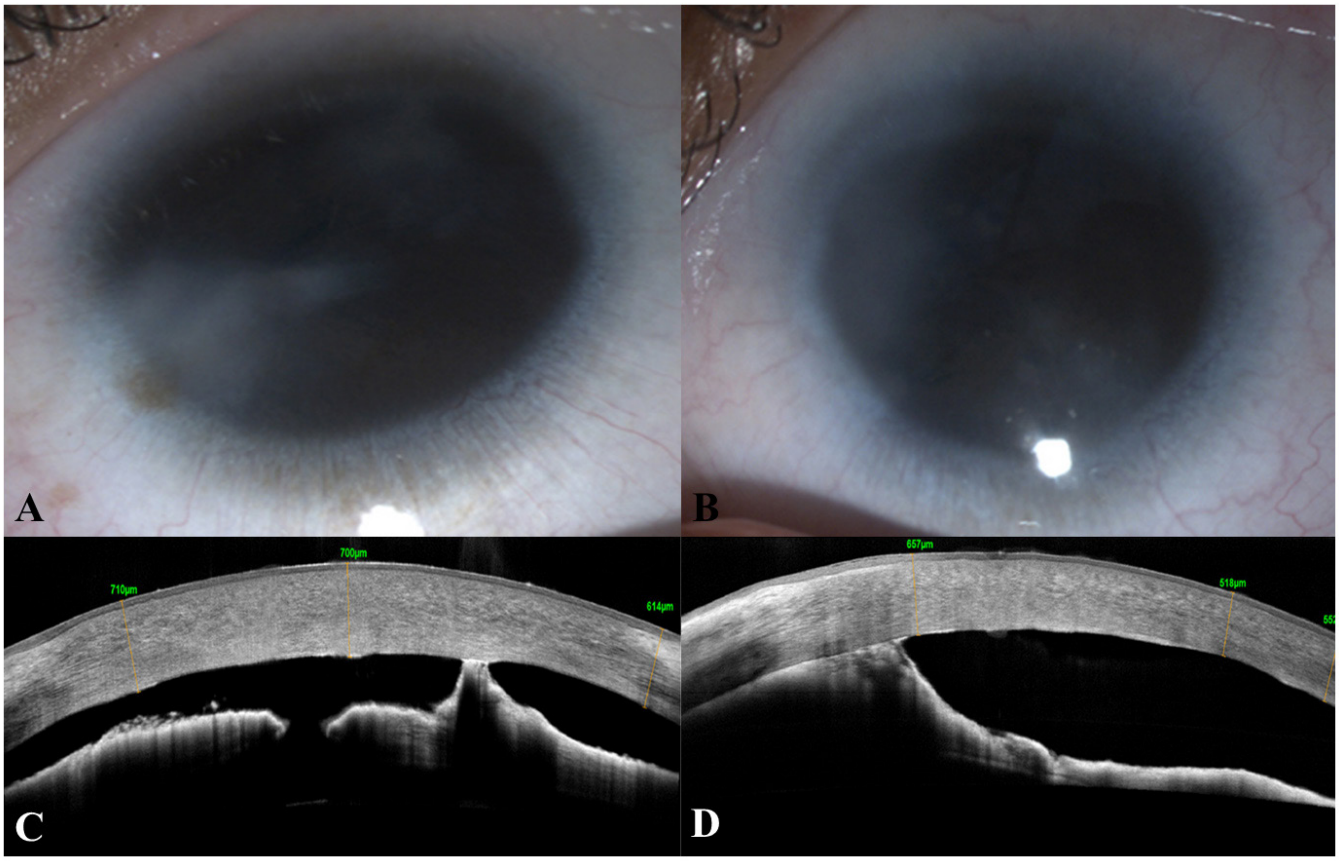


Figure 2. Representative clinical images of CP1 in each eye. **A**, **B**: Slit-lamp photographs show markedly flattened corneal curvature and diffuse stromal haze with a ground-glass opacity. The limbal architecture appears indistinct, blending with the sclera. The pupil is poorly visualized due to stromal opacity. **C**, **D**: Anterior segment optical coherence tomography (AS-OCT) cross-sectional images reveal marked corneal flattening with reduced anterior curvature. The cornea appears thickened centrally relative to the periphery. There is a significantly shallow anterior chamber, with anteriorly displaced iris tissue and iridocorneal adhesions, indicating abnormal anterior segment configuration. The angle appears compromised, predisposing to angle-closure mechanisms. Stromal reflectivity is increased, corresponding to corneal haze.

confocal microscopy in recessive CP. In contrast, our study used both AS-OCT and UBM to comprehensively assess the anterior chamber, including iris insertion. AS-OCT allowed precise quantification of severe corneal flattening, pachymetry, and markedly shallow anterior chamber depth, as well as evaluation of the iris–cornea relationship. On the other hand, UBM showed a detailed visualization of anterior chamber configuration, angle anatomy, and ciliary body position, detecting anterior rotation, lens displacement, and structural risk factors for angle closure. Both provided a complete picture for diagnosis and glaucoma risk assessment in CP [13]. Additional complications, including elevated intraocular pressure secondary glaucoma, endothelial decompensation, and cataract formation, have been reported in some cases, emphasizing the progressive nature and multisystemic impact of the disease within the eye [14-17]. However, the corneal endothelium, analyzed in one case (CP5a) in our study, had a normal morphology (Figure 3).

Among the six identified *KERA* variants, two were novel and had not been previously reported in patients with CP. Among the reported variants, the p.Arg313Ter variant is considered a recurrent stop-gain mutation [10,17,18], and p.Arg279Ter has been described in multiple studies [2,7,10,16,19]. The variants p.Ser270Leu and p.Asn176Lys were identified in a UK-based multiethnic cohort from the 100,000 Genomes Project, in which two patients with the CP phenotype harbored these variants [20]. Pellegata et al. [7] found 46 Finnish patients homozygous for a single founder missense *KERA* mutation, c.740A>G (p.Asn247Ser). In a cohort of five CP cases from Czech and Turkish populations, Czech probands carried either compound heterozygous variants (c.209C>T; p.(Pro70Leu); c.887–1G>A) or the recurrent

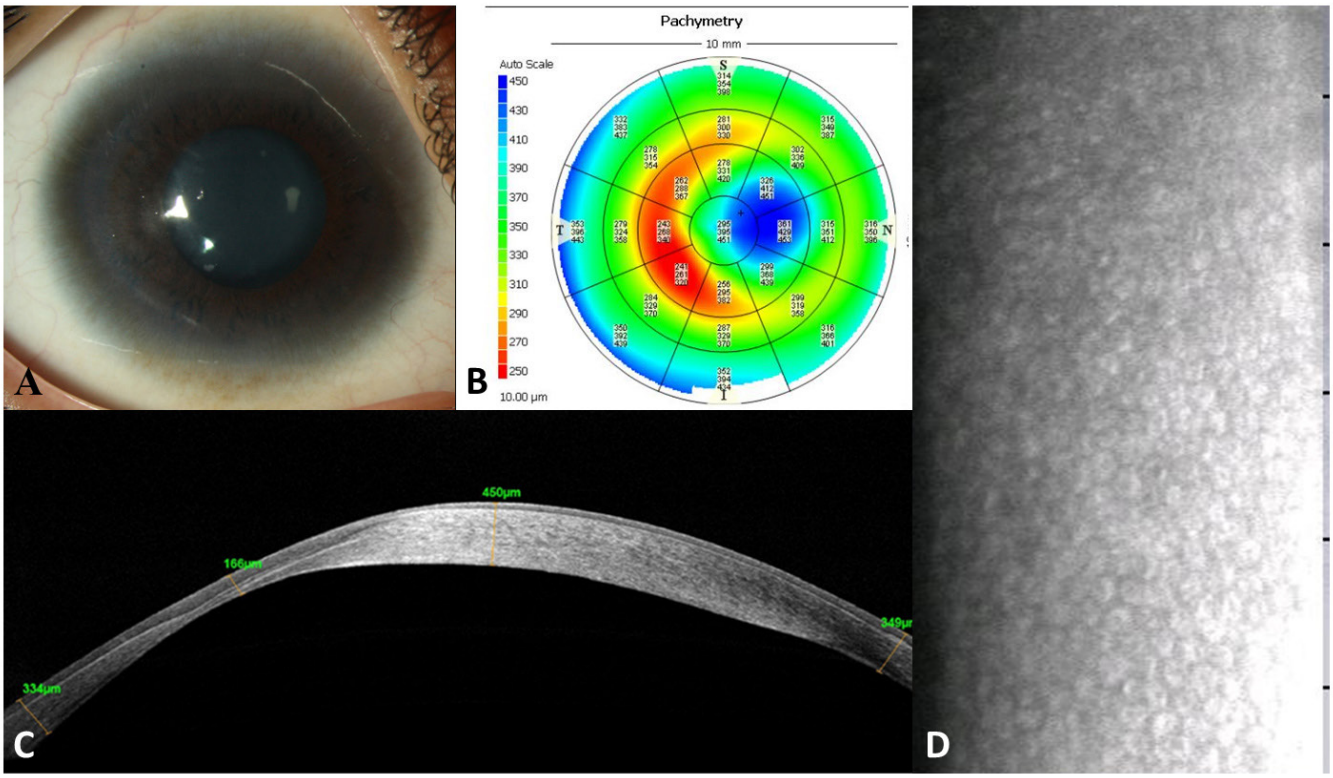


Figure 3. Representative clinical images of the right eye of CP5a. **A**: Slit-lamp photograph shows diffuse stromal haze with a ground-glass appearance, markedly flattened corneal curvature, and indistinct limbal architecture. **B**: Pachymetry map demonstrates an abnormal corneal thickness profile with relative central thickening and peripheral thinning. **C**: Anterior segment optical coherence tomography (AS-OCT) image shows reduced corneal curvature and central corneal thickness of approximately 450 µm, a thinner peripheral cornea, and a shallow anterior chamber. Fine iris details are limited, but imaging suggests anterior iris insertion toward the posterior corneal surface. **D**: Specular microscopy image shows preserved endothelial cell morphology without significant pleomorphism or polymegathism.

homozygous nonsense variant c.835C>T (p.Arg279*), while Turkish probands had homozygous missense variants c.740A>G (p.Asn247Ser) or c.674C>T (p.Ile225Thr), with c.740A>G being the most recurrent *KERA* mutation across populations [19]. Importantly, our genetic findings highlight the considerable allelic heterogeneity of *KERA*. All cases had different *KERA* variants localized to different exonic regions of the *KERA* gene, suggesting that pathogenic alterations across multiple domains can disrupt corneal morphogenesis (Figure 5A).

Notably, in the CP5 pedigree, the clinical history initially suggested an autosomal dominant pattern of inheritance owing to multiple affected members. However, genetic analysis revealed that the proband harbored a homozygous *KERA* variant c.528C>G (p.Asn176Lys), indicating an autosomal recessive form of CP. The corresponding clinical phenotypes were also consistent with those of autosomal recessive CP. This observation raises the possibility of pseudo-dominant inheritance in this family, a pattern that, to our knowledge, has not been previously reported in CP. Nonetheless, a comprehensive segregation analysis involving both affected and unaffected family members is required to substantiate this hypothesis. Collectively, these findings expand the clinical and allelic spectrum of *KERA*-associated CP.

Given the genetic basis and early-onset nature of CP, genetic testing should be considered integral to the diagnostic workup, particularly in patients with atypical anterior segment features or in populations with a high prevalence of consanguineous marriages. Molecular confirmation not only aids in diagnosis but also provides a basis for genetic counseling and reproductive planning, especially in families with multiple affected individuals. Furthermore, improved characterization of variant pathogenicity through large-scale registries and functional validation may refine our prognostic understanding and identify potential therapeutic targets.

Management plans in CP remain largely supportive, with primary emphasis on optimal refractive correction. Surgical interventions may be considered in selected cases with

Table 2. Characteristic features of *KERA* variants identified in six CP probands.

Proband	CP1	CP2	CP3	CP4	CP5	CP6
Consanguinity	Y	Y	NO	Y	Y	Y
Type of Variants	Frameshift	Frameshift	Missense	Stop-gain	Missense	Stop-gain
Zygosity/Inheritance	Homo/AR	Homo/AR	Homo/AR	Homo/AR	Homo/AR	Homo/AR
***KERA* c. DNA Variant**	c.264_298del	c.59_78delinsA	c.809C>T	c.937C>T	c.528C>G	c.835C>T
***KERA* Protein Variant**	p.Glu88Aspfs*14	p.Ser20TyrfsTer57	p.Ser270Leu	p.Arg313Ter	p.Asn176Lys	p.Arg279Ter
Exon	2	2	2	3	2	2
WES Coverage	45X	28X	50X	37X	33X	27X
Pathogenicity ACMG	Likely pathogenic PM2 & PVS1	Likely pathogenic PM2 & PVS1	Uncertain Significance PM2 & PP3	Likely pathogenic PM2, PVS1 & PP5	Uncertain significance PM2 & PP3	pathogenic PM2,PVS1 and PP5
Status	Novel	Novel	Reported	Reported	Reported	Reported
db SNP ID	-	-	rs764245015	rs121917863	rs781367942	rs386833986
SIFT Score	-	-	0	-	0	-
NMD	Yes	Yes		NMD escape		NMD escape
PolyPhen Score	-	-	0.962	-	1	-
CADD Score	-	-	28.3	-	18.4	-
Mutation Taster prediction	Deleterious	Deleterious	Deleterious	Deleterious	Deleterious	Deleterious
Predicted Protein stability change			mCSM (ΔΔG): −0.16 kcal/mol (Destabilizing)		SDM (ΔΔG): −1.33 kcal/mol (Destabilizing)	

The table includes identified *KERA* variants in 6 CP probands with variant nomenclature, mutation type, zygosity, variant status, ACMG classification, in silico predictions outcomes and novelty status based on reference databases and literature review.

residual refractive error, including photorefractive keratectomy and laser thermal keratoplasty, laser in situ keratomileusis, or conductive keratoplasty. While surgical interventions may provide limited benefit in selected cases, their overall role remains restricted due to the underlying structural abnormalities of the cornea and variable visual outcomes [21]. In our cohort, treatment strategies included hyperopic refractive correction, amblyopia therapy, and selective anterior segment reconstruction. The surgical interventions were performed primarily for visual rehabilitation and prevention of complications. Refractive correction with glasses or contact lenses is often challenging due to extreme hyperopia and corneal irregularities. Additionally, lenticular changes such as cataracts require individualized surgical planning, with intraocular lens selection carefully tailored to the unique anterior segment anatomy and refractive needs [22]. In cases of dense central corneal opacities, surgical interventions such as corneal transplantation remain inadequately established in CP. The outcomes of keratoplasty are often limited by underlying anatomic challenges, including reduced corneal thickness, shallow anterior chamber depth, and significant irregular astigmatism, which collectively compromise graft success and visual rehabilitation [23]. These challenges underscore the importance of early diagnosis and multidisciplinary management to optimize visual outcomes.

Overall, this study broadens the clinical and genetic landscape of *KERA*-associated CP in an Indian cohort. A key limitation of this study is that the identified variants were not validated by Sanger sequencing but were instead inferred from whole-exome sequencing reports and phenotypic concordance. However, identifying two novel *KERA* variants and one instance of pseudo-dominant inheritance highlights the importance of a comprehensive genetic evaluation. These findings underscore the value of early genetic testing and detailed ophthalmic evaluation in guiding patient management. Given the lack of effective treatments, further research is warranted to explore targeted therapeutic options.

ACKNOWLEDGMENTS

We would like to acknowledge patients and their families for their participation and Hyderabad Eye Research Foundation (HERF) and Hyderabad Eye Institute (HEI) for institutional funding support. Conflict of interests: The authors declare that there is no conflict of interest. Financial support:

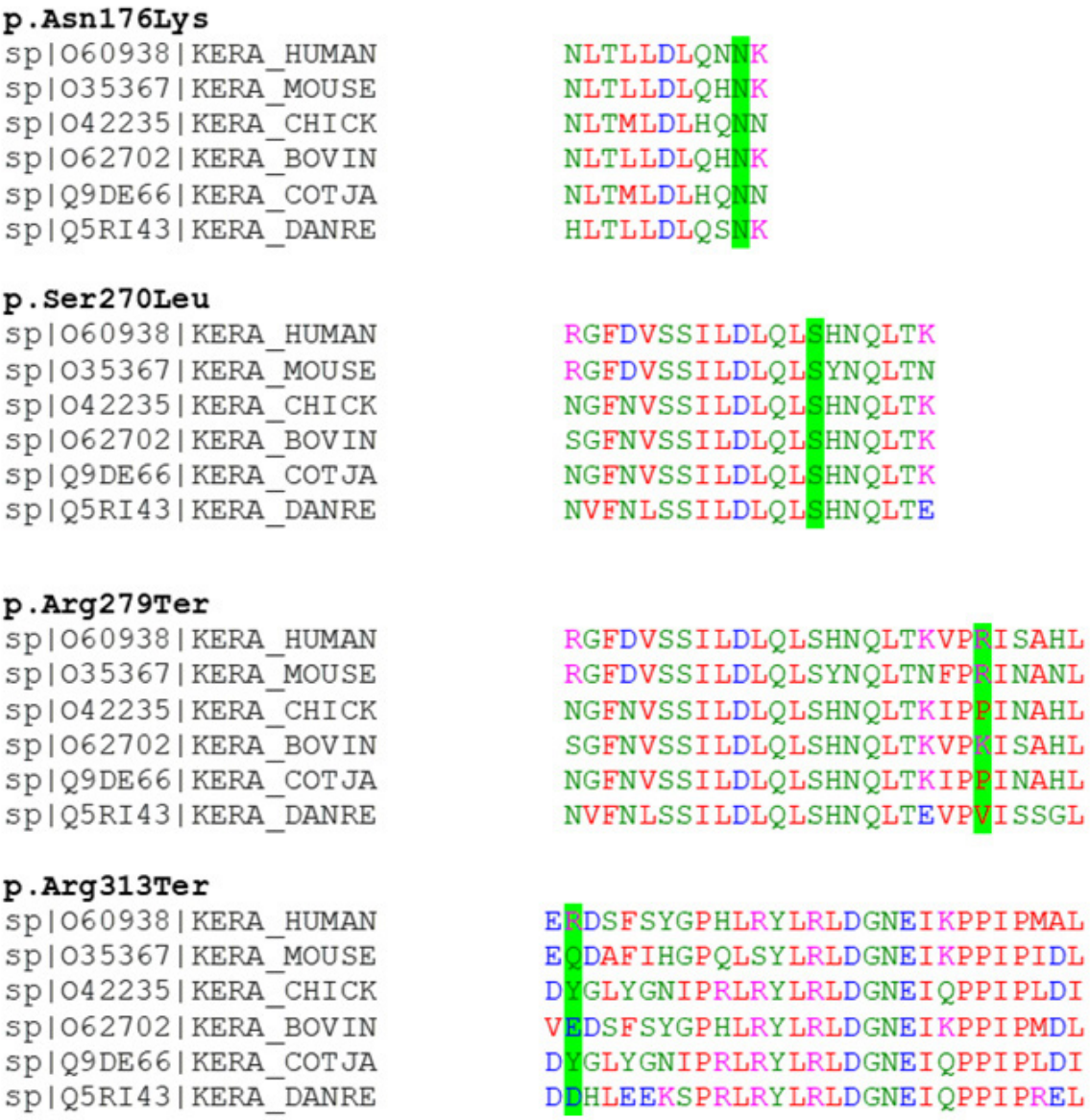


Figure 4. Conservation analysis of KERA protein across six orthologous species. Missense variants p.Asn176Lys and p.Ser270Leu affect highly conserved residues, whereas the nonsense variants p.Arg279Ter and p.Arg313Ter are located in less conserved regions.

Hyderabad Eye Research Foundation and Hyderabad Eye Institute, Hyderabad, India. Financial Disclosure (s): The authors have no proprietary or commercial interest in any materials discussed in this article. Author's Role: Involved in the design and conduct of the study (MDR); data collection (AV, SPG, MDR); analysis and interpretation of results (AV, MDR, SCH, DE); preparation of the manuscript and literature search (AV, MDR, SPG, DE); review of the manuscript (AV, MDR, DE); final approval (MDR).

This is an open-access article distributed under the terms of the Creative Commons Attribution-NonCommercial-NoDerivatives 4.0 International License, which permits reusers to copy and distribute the material in any medium or format in unadapted form only, for noncommercial purposes only, and only so long as attribution is given to the creator. CC

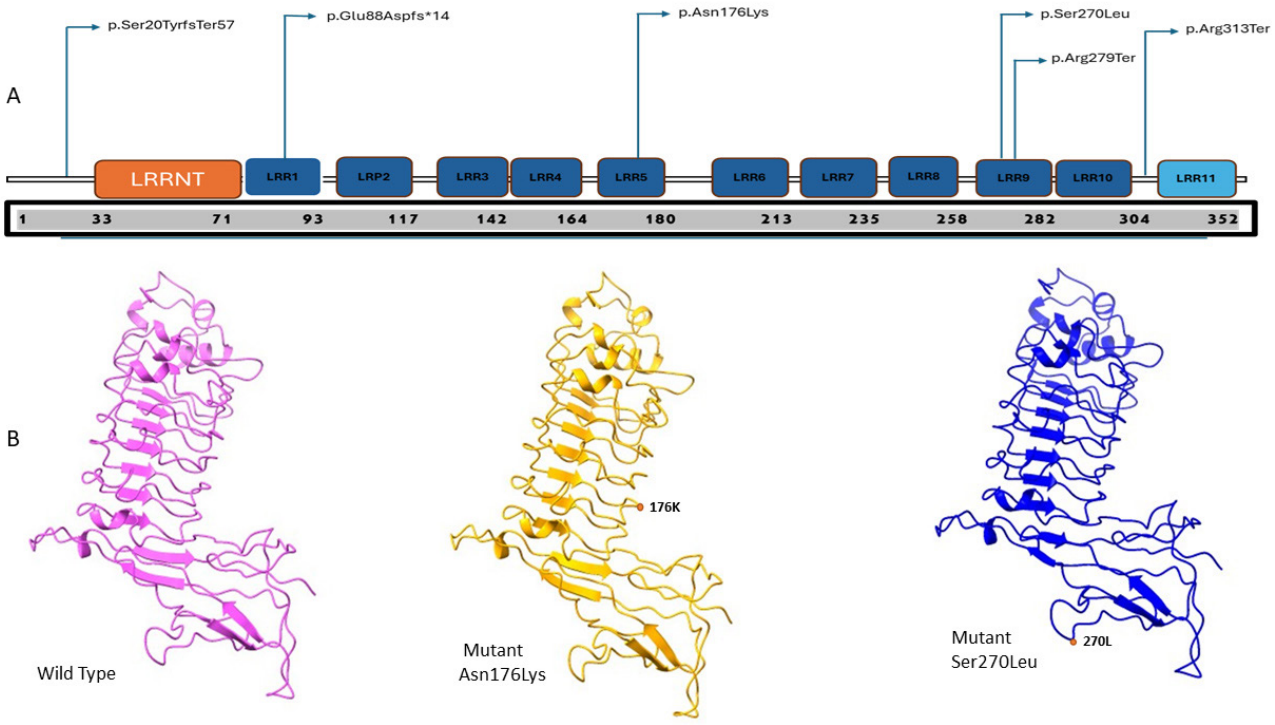


Figure 5. Schematic representation and three-dimensional structure of the keratocan protein. **A**: This panel shows the structural organization of keratocan, which consists of one leucine-rich repeat N-terminal (LRRNT) domain and 11 leucine-rich repeat (LRR) domains composed of alternating α-helices and β-sheets. The positions of the six identified KERA variants are indicated according to their amino acid locations within the protein domains. **B**: This panel shows the three-dimensional structures of the wild-type KERA protein and the mutant p.Asn176Lys and p.Ser270Leu proteins. The mutant proteins exhibit minimal global structural deviations from the wild-type protein, with root mean square deviation values of 0.188 Å and 0.204 Å, respectively, indicating preservation of the overall protein fold.

BY-NC-ND includes the following elements: BY: credit must be given to the creator. NC: Only noncommercial uses of the work are permitted. ND: No derivatives or adaptations of the work are permitted.

REFERENCES

1. Forsius H, Damsten M, Eriksson AW, Fellman J, Lindh S, Tahvanainen E. Autosomal recessive cornea plana. A clinical and genetic study of 78 cases in Finland. Acta Ophthalmol Scand 1998; 76:196-203. [PMID: 9591953].

2. Huang C, Long X, Peng C, Lin P, Tan H, Lv W, Wu L. Novel variants in the KERA gene cause autosomal recessive cornea plana in a Chinese family: A case report. Mol Med Rep 2019; 19:4711-8. [PMID: 31059048].

3. Tahvanainen E, Villanueva AS, Forsius H, Salo P, de la Chapelle A. Dominantly and recessively inherited cornea plana congenita map to the same small region of chromosome 12. Genome Res 1996; 6:249-54. [PMID: 8723718].

4. Shorb SR. Bilateral ametropic amblyopia resulting from bilateral cornea plana. Am J Ophthalmol 1972; 73:663-4. [PMID: 5028981].

5. Fay J, Herzlich AA, Florakis GJ. Posterior amorphous corneal dystrophy associated with keratoglobus: a case report. Cornea 2017; 36:1562-6. [PMID: 28902010].

6. Cameron JA. Corneal abnormalities in Ehlers-Danlos syndrome type VI. Cornea 1993; 12:54-9. [PMID: 8458232].

7. Pellegata NS, Dieguez-Lucena JL, Joensuu T, Lau S, Montgomery KT, Krahe R, Kivelä T, Kucherlapati R, Forsius H, de la Chapelle A. Mutations in KERA, encoding keratocan, cause cornea plana. Nat Genet 2000; 25:91-5. [PMID: 10802664].

8. Gesteira TF, Verma S, Coulson-Thomas VJ. Small leucine rich proteoglycans: Biology, function and their therapeutic potential in the ocular surface. Ocul Surf 2023; 29:521-36. [PMID: 37355022].

9. Liu CY, Birk DE, Hassell JR, Kane B, Kao WWY. Keratocan-deficient mice display alterations in corneal structure. J Biol Chem 2003; 278:21672-7. [PMID: 12665512].

10. Khan AO, Aldahmesh M, Meyer B. Recessive cornea plana in the Kingdom of Saudi Arabia. Ophthalmology 2006; 113:1773-8. [PMID: 17011957].

11. Sigler-Villanueva A, Tahvanainen E, Lindh S, Dieguez-Lucena J, Forsius H. Autosomal dominant cornea plana: clinical findings in a Cuban family and a review of the literature. Ophthalmic Genet 1997; 18:55-62. [PMID: 9228241].

12. Bruni E, Pedrotti E, Sarro PPD, Passilongo M, Marchini G. *In vivo* confocal microscopy of iris in recessive cornea plana with anterior synechiae. Indian J Ophthalmol 2018; 66:1311-3. [PMID: 30127149].

13. Raja V, Tara T, Kondepati K, Senthilkumar V. Multimodal imaging of autosomal recessive cornea plana associated with hard mature and polar cataract. Indian J Ophthalmol Case Rep 2021; 1:393-4. .

14. Kumari D, Tiwari A, Choudhury M, Kumar A, Rao A, Dixit M. A Novel KERA Mutation in a Case of Autosomal Recessive Cornea Plana With Primary Angle-Closure Glaucoma. J Glaucoma 2016; 25:e106-9. [PMID: 25967529].

15. Abdalla Elsayed MEA, MacLaren RE. Cataract surgery with autosomal recessive cornea plana caused by a novel *KERA* mutation. Am J Ophthalmol Case Rep 2026; 41:102514[PMID: 41550454].

16. Dudakova L, Palos M, Hardcastle AJ, Liskova P. Corneal endothelial findings in a Czech patient with compound heterozygous mutations in KERA. Ophthalmic Genet 2014; 35:252-4. [PMID: 23834557].

17. Khan AO, Aldahmesh MA, Al-Gehedan S, Meyer BF, Alkuraya FS. Corneal decompensation in recessive cornea plana. Ophthalmic Genet 2009; 30:142-5. [PMID: 19941419].

18. Khan A, Al-Saif A, Kambouris M. A novel KERA mutation associated with autosomal recessive cornea plana. Ophthalmic Genet 2004; 25:147-52. [PMID: 15370545].

19. Dudakova L, Vercruyssen JHJ, Balikova I, Postolache L, Leroy BP, Skalicka P, Liskova P. Analysis of *KERA* in four families with cornea plana identifies two novel mutations. Acta Ophthalmol 2018; 96:e87-91. [PMID: 28677912].

20. Jackson D, Malka S, Harding P, Palma J, Dunbar H, Moosajee M. Molecular diagnostic challenges for non-retinal developmental eye disorders in the United Kingdom. Am J Med Genet C Semin Med Genet 2020; 184:578-89. [PMID: 32830442].

21. Khan TA, Zameer S, Janjua TA, Zahid MA, Akram A, Mallick NK. Cornea plana in a family from Pakistan: Case series and literature review on the principles of management. Oman J Ophthalmol 2023; 16:305-9. [PMID: 37602180].

22. Fogla R, Indumathy TR. Customized toric intraocular lens implantation in cornea plana. J Cataract Refract Surg 2020; 46:e11-4. [PMID: 32818351].

23. Park B, Ziari M, Castro HM, Ali SF. A Review of Pediatric Corneal Transplants: Perioperative, Operative, and Postoperative Management. Int Ophthalmol Clin 2022; 62:15-31. [PMID: 34965223].

Articles are provided courtesy of Emory University and The Abraham J. & Phyllis Katz Foundation. The print version of this article was created on 20 September 2026. This reflects all typographical corrections and errata to the article through that date. Details of any changes may be found in the online version of the article.